Diastereomeric Salt Crystallization Synthesis for Chiral Resolution of Ibuprofen

Wai H. Lam and Ka M. Ng
Dept. of Chemical Engineering, Hong Kong University of Science and Technology, Clear Water Bay, Hong Kong

DOI 10.1002/aic.11087
Published online January 2, 2007 in Wiley InterScience (www.interscience.wiley.com).

Conceptual design and experimental investigations are integrated for synthesizing diastereomeric salt crystallization processes for chiral resolution. An anti-inflammatory drug ibuprofen and a common resolving agent N-methyl-D-glucamine were chosen to illustrate this integrative approach. Bench data were generated in a systematic manner. Solvent screening was conducted first to identify the right solvent to precipitate the diastereomeric salts. Solid–liquid equilibrium data of the diastereomeric salt system were then measured. Seeding was used to facilitate the precipitation of the desired component. All of this information was used to generate flow sheet alternatives to recover the desired diastereomeric salts. © 2007 American Institute of Chemical Engineers *AIChE J,* 53: 429–437, 2007
Keywords: ibuprofen resolution, diastereomeric salt crystallization processes, solid–liquid equilibrium phase diagram, seeding, process synthesis

Introduction

Diastereomeric salt crystallization processes (DSCPs) are the most widely used methods to separate chiral compounds. It was estimated that more than half of the chiral drugs in the market were produced through DSCP.[1] In this process, the racemic acid or base reacts with a resolving agent, an optically active base or acid, to form a pair of diastereomeric salts. Differences in solubility and crystallization rate of these salts form the basis of separation by crystallization. After recovering the desired diastereomeric salt, it can be decomposed to liberate the corresponding enantiomer by treating it with a strong acid or base.

Ibuprofen (IBU), a candidate for using DSCP, belongs to a class of nonsteroidal anti-inflammatory drugs widely used to relieve a range of general inflammatory conditions.[2] It has been sold in racemic dosage form but research findings showed that (S)-IBU exhibited superior performance compared with the racemate.[3] The commercial potential has led to extensive research efforts in developing DSCP for ibuprofen. Common resolving agents such as (S)-lysine[4–6] and *N*-methyl-D-glucamine (NMDG)[7] were used to resolve the chiral compound. Nohira[8] developed a designer amine specifically for ibuprofen resolution. These reported resolutions were mainly conducted by seeding in supersaturated solution. As indicated by Bhattacharya,[6] the desired diastereomeric salt formed between (S)-lysine and (S)-ibuprofen could not be recovered under equilibrium conditions because it was the more soluble salt species. However, it was successfully recovered by seeding at low temperature, indicating that crystallization of the desired diastereomeric salt was more kinetically favorable. A significant amount of effort was expended on determining the conditions—such as crystallization temperature, solution concentration, resolving agent to racemate ratio, and crystallization time—that achieved the highest yield of pure enantiomers. Design by exhaustive search is typical in chiral resolution by the seeding method.[9]

A systematic framework to develop DSCP under equilibrium conditions was proposed by Schroer et al.[10] With the aid of a solid–liquid equilibrium (SLE) phase diagram, feasible DSCP can be identified. The recovered salt species does not have to be the less soluble one. If there are favorable changes in phase behavior under different temperatures or racemate to resolving agent ratios, it is possible to recover the more soluble species under equilibrium conditions.

This work aims at developing an integrative approach to identify diastereomeric salt crystallization process alternatives. It involves four steps: (1) solvent screening, (2) mea-

Correspondence concerning this article should be addressed to K. M. Ng at kekmng@ust.hk.

surement of SLE phase diagrams, (3) crystallization by seeding, and (4) process synthesis. The rationale, experimental approach, and process synthesis will be demonstrated using ibuprofen with NMDG as the resolving agent.

An Integrative Approach

Solvent screening

Solvent selection is very important for diastereomeric salt formation. Many solvents are not able to induce the crystallization of the diastereomeric salts. For example, oils instead of crystals are obtained upon solvent evaporation.[11] Another possible problem is that the solubility of the salts is too high in the selected solvent. A high concentration of solute in a saturated solution is not conducive to the formation of good quality crystals. Also, the viscosity of such a concentrated solution can be so high that it hinders precipitation. For all of these reasons, screening as described below is essential for solvent selection.[9,12]

In this study, five solvents were chosen for screening: water, ethanol, isopropyl alcohol, acetone, and ethyl acetate. An amount of 0.206 g of (S)-IBU (10^{-3} mole) was dissolved in 0.5 mL of each solvent. The solutions were stirred until complete dissolution. Similarly, 0.195 g of NMDG (10^{-3} mole) was dissolved in 0.5 mL of each solvent. The ibuprofen solution and the NMDG solution with the same solvent were then mixed together. The five mixtures were heated in a water batch at 50°C with stirring. In the case of ethyl acetate, a homogeneous solution could not be obtained even after further heating to 70°C. In any event, the resulting solutions were placed inside a sonication bath to promote mixing, which in turn was connected to a water bath for temperature control (Figure 1). The solutions were cooled to 8°C under sonication. Solids precipitated out only from a homogeneous solution of acetone. These solid precipitates were filtered and dried in a vacuum oven at 40°C overnight. The dried solids were characterized using a differential scanning calorimeter (Texas Instrument 2910). After equilibration for 5 min at 30°C, ramping was carried out from 30 to 250°C at 5°C/min. The solids were also analyzed using high-performance liquid chromatography (HPLC). The column was an Xterra® MS C_{18} (Waters Chromatography Division/Millipore, Milford, MA) and the mobile phase was 0.1 vol % H_3PO_4 in methanol. The flow rate was 1 mL/min under gradient mode.

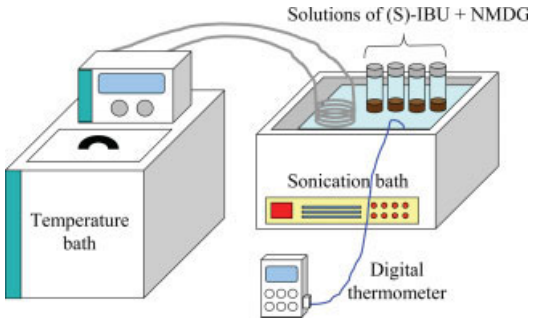

Figure 1. Schematic of the sonication-temperature control unit.

[Color figure can be viewed in the online issue, which is available at www.interscience.wiley.com.].

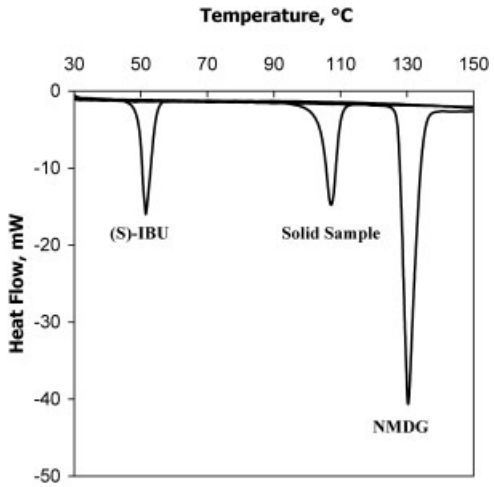

Figure 2. DSC thermalgram of the solid sample.

A differential scanning calorimetric (DSC) thermalgram of the solid sample, (S)-IBU, and NMDG is shown in Figure 2. The melting point of the solid sample was 106.7°C, which was different from that of (S)-ibuprofen (51°C) and NMDG (130°C). It can be deduced that the solid sample must be a new chemical species. The composition of the solid sample was analyzed using HPLC. The molar ratio of (S)-IBU to NMDG was 0.99:1.00, indicating an equimolar mixture of ibuprofen and NMDG. Combining the results of both DSC and HPLC, it is certain that the solid sample from the acetone solution must be the diastereomeric salt formed between (S)-IBU and NMDG, hereafter referred to as NMDG-IBU.

Measurement of SLE phase diagrams

The SLE phase diagram is the most complete representation of phase behavior. By showing how the behavior changes under the influence of temperature and composition, it provides a convenient vehicle for visualizing how to recover a pure component by changing process conditions. Indeed, a systematic procedure for synthesizing equilibrium-based crystallization processes is available.[13]

In this work, it is of interest to study the SLE phase behavior of the diastereomeric salts, NMDG-(S)-IBU and NMDG-(R)-IBU, in acetone under isobaric–isothermal conditions. In addition, the effects of nonstoichiometric use of resolving agent on the SLE phase behavior are also considered. The system under consideration is an electrolyte solution because ibuprofen and NMDG undergo ionic dissociation to form diastereomeric salts:

$$\text{(S)-IBU} \leftrightarrow \text{(S)-IBU}^- + \text{H}^+ \quad (1)$$

$$\text{(R)-IBU} \leftrightarrow \text{(R)-IBU}^- + \text{H}^+ \quad (2)$$

$$\text{NMDG} + \text{H}^+ \leftrightarrow \text{NMDG-H}^+ \quad (3)$$

$$\text{NMDGH}^+ + \text{(S)-IBU}^- \leftrightarrow \text{NMDG-(S)-IBU} \quad (4)$$

$$\text{NMDGH}^+ + \text{(R)-IBU}^- \leftrightarrow \text{NMDG-(R)-IBU} \quad (5)$$

Schroer et al.[10] showed that, under stoichiometric use of resolving agent, both racemate and resolving agent often undergo

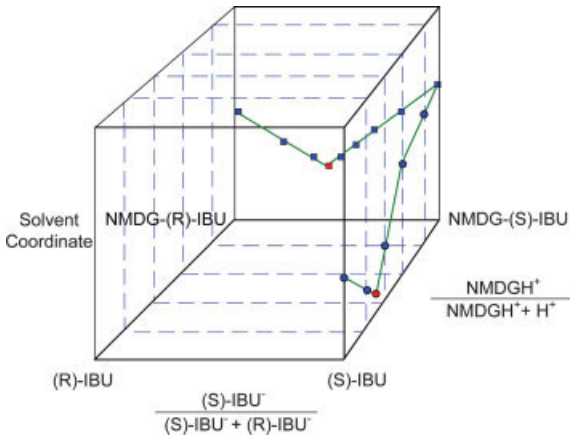

Figure 3. Dividing the composition space into a series of planes for determining the isobaric isothermal phase diagram.

[Color figure can be viewed in the online issue, which is available at www.interscience.wiley.com.]

nearly complete dissociation (>99%). However, it is not uncommon to use a nonstoichiometric amount of resolving agent on chiral resolutions by diastereomeric salt crystallization.[9,12] In this case, the effect of the resolving agent to racemate molar ratio (R) on the SLE behavior of the system becomes important. Consider the situation where there is more racemate than resolving agent on a molar basis in the solution. If there are no solvates or unexpected compounds, there will be five salt species that can precipitate out from the solution: the two diastereomeric salts, NMDG-(S)-IBU and NMDG-(R)-IBU; two enantiomers, (S)-IBU and (R)-IBU; and the racemic compound formed between the two enantiomers, referred to as (S)-IBU-(R)-IBU.

According to Samant and Ng,[14] three coordinates are required to construct the phase diagram of this quaternary reciprocal salt pairs system under isobaric–isothermal conditions: cationic, anionic, and solvent coordinates. If NMDG-H^+ and (S)-IBU^- are chosen as the bases for the cationic and anionic coordinates, respectively, we have

$$\text{Cationic coordinate}, Y = \frac{[\text{NMDGH}^+]}{[\text{NMDGH}^+ + \text{H}^+]} \tag{6}$$

$$\text{Anionic coordinate}, X = \frac{[(\text{S})\text{-IBU}^-]}{[(\text{S})\text{-IBU}^- + (\text{R})\text{-IBU}^-]} \tag{7}$$

$$\text{Solvent coordinate} = \frac{\text{Volume of solvent (ml)}}{\text{Amount of solute (g)}} \tag{8}$$

It should be noted that the cationic coordinate actually represents the resolving agent to racemate ratio. A cationic coordinate value of one represents the stoichiometric use of resolving agent and zero corresponds to the enantiomeric system.

To construct the desired isobaric–isothermal phase diagram, the saturation compartment of each salt species has to be located. The double saturation curves separate neighboring compartments. By determining the locations of a sufficient number of double saturation points, the double saturation curves and thus the saturation compartments can be fixed.

Fuyuhiro et al.[15] constructed the isobaric–isothermal phase diagram of the reciprocal salt pairs system of optically active cobalt (III) complexes by measuring the double saturation points directly. They put an excess amount of solutes into the solution and then measured the solubility at equilibrium.

Here, an indirect approach was used to locate the double saturation points. First, the phase diagram was divided into a series of planes along the cationic coordinate such that the cationic composition was fixed at $Y = 0$, 0.2, 0.4, 0.6, 0.8, and 1 (Figure 3). An imaginary solubility curve of the diastereomeric salt system at $Y = 1$ is shown for illustration. By measuring the solubility data points (in blue) along each plane, the double saturation point (in red) can be located by extrapolation. Similarly, solubility data were taken in each plane of $X = 0.05$, 0.2, 0.3, 0.4, 0.5, 0.6, 0.8, and 1. The solubility data in this work were measured using about 0.3 g of solids at 35°C using the isothermal method.[16] Basically the solids were dissolved with a sufficient amount of solvent and homogenized at 40°C for 5 min. This was followed by cooling the solution to about 15–20°C to initiate solid precipitation. Once solids started to accumulate, the solutions were reheated to 35°C and solvent was added periodically until all solids dissolved. The solvent was a 95% acetone and 5% water mixture by volume.

The locations of the double saturation points are plotted on a Jänecke projection (Figure 4). Squares represent the double saturation points obtained along the cationic coordinates; circles represent those obtained along the anionic coordinates. Compartment boundaries are obtained by connecting the double saturation points. Five saturation compartments can be identified: those of NMDG-(R)-IBU, NMDG-(S)-IBU, (R)-IBU-(S)-IBU, (R)-IBU, and (S)-IBU. Based on the solubility data[17] and the predicted boundaries, a complete isobaric–isothermal phase diagram of the diastereomeric salt

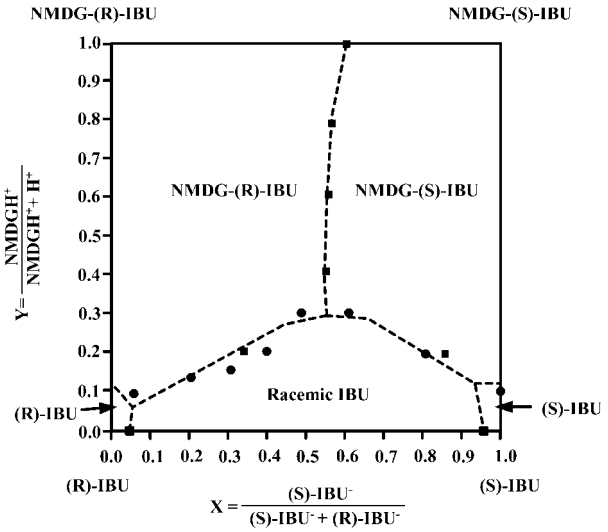

Figure 4. Location of the double saturation points, along with the double saturation curves and crystallization compartments, on a Jänecke projection.

Squares represent the double saturation points obtained along the cationic coordinates; circles represent those obtained along the anionic coordinates.

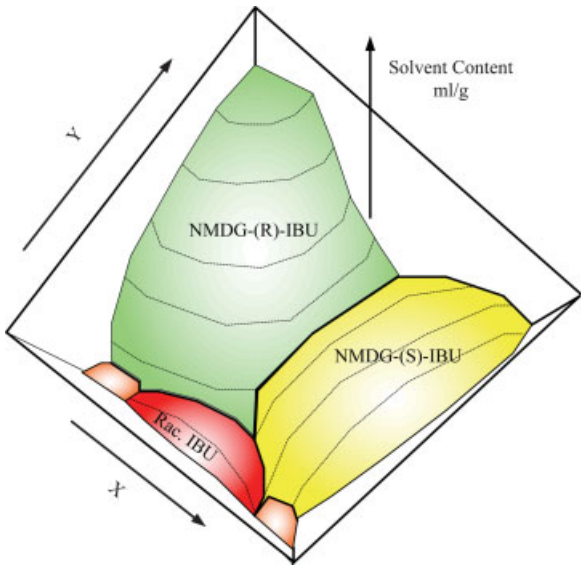

Figure 5. Isobaric isothermal solid–liquid equilibrium phase diagram of the diastereomeric salt system of NMDG and ibuprofen.

[Color figure can be viewed in the online issue, which is available at www.interscience.wiley.com.]

system formed between ibuprofen and NMDG is sketched in Figure 5.

It can be seen that the undesirable diastereomeric salt, NMDG-(R)-IBU, is less soluble than the desired one, NMDG-(S)-IBU, as indicated by the relative size of the respective saturation compartment. The double saturation point shifted slightly from $X = 0.59$ to $X = 0.55$ as Y changed from 1 to 0.4 with the changing amount of resolving agent. In this acetone–water solvent, the solubility of the enantiomers and the racemic compound is much higher than that of the diastereomeric salts. They do not precipitate out at a resolving agent to racemate ratio ~ 0.3.

Crystallization by seeding

Growth of NMDG-(S)-IBU crystals was initiated by introducing seeds of NMDG-(S)-IBU into a supersaturated solution. Crystallization was allowed to proceed even after nuclei of NMDG-(R)-IBU started to form. The induction period—the time lag between the onset of supersaturation and formation of critical nuclei—can be used as a measure of the allowable seeding time. The length of induction period decreases with increasing temperature and supersaturation ratio S, defined as

$$S = \frac{c}{c^*} \tag{9}$$

where c is the solute concentration and c^* is the saturation concentration at the given temperature.[18,19]

With a high supersaturation ratio, the induction period is short. However, a higher yield can be obtained because of the larger amount of solute in excess of that in a saturated solution. In addition, crystals grow faster at higher supersaturation. By studying the influences of supersaturation ratio and temperature on the induction period, optimal conditions can be identified to conduct the seeding experiment. However, because of the change in solution composition during crystallization, nuclei of NMDG-(R)-IBU may form within the induction period. This can affect the crystal purity as crystals of NMDG-(R)-IBU can start to grow. Therefore, it is also important to monitor the solid purity during the crystallization.

A review of the literature shows that most of the seeding experiments were attempted on a supersaturated solution with an equimolar mixture of the two diastereomeric salts. However, because the target diastereomeric salt NMDG-(S)-IBU is more soluble than the undesirable one, it may be more desirable to conduct the seeding experiment in a supersaturated solution with composition at the double saturation point. This solution is richer in the desired salt (~59% NMDG-(S)-IBU) than a solution of equimolar composition. It can be prepared by first crystallizing and filtering out the undesirable diastereomeric salt until the double saturation point is reached and then lowering the temperature to create a supersaturated solution.

Supersaturated solutions of S equal to 1.5, 1.8, 2, and 2.5 at 5 and 35°C were prepared to study the influence of supersaturation ratio and temperature on induction period. The temperature was raised to 5°C above their dissolution temperature to ensure solution homogeneity. Then, each solution was cooled to the desired temperature at a ramping rate of −0.7°C/min. Time counting was started when the solution reached the desired temperature and stopped when small nuclei were observed by unaided naked eyes. The time difference was recorded as the induction period.

In the seeding experiments, supersaturated solutions of double saturation composition and equimolar composition were prepared. Again, the solutions were cooled to the desired seeding temperature at a ramping rate of −0.7°C/min. Seeds of NMDG-(S)-IBU were introduced into the solution and

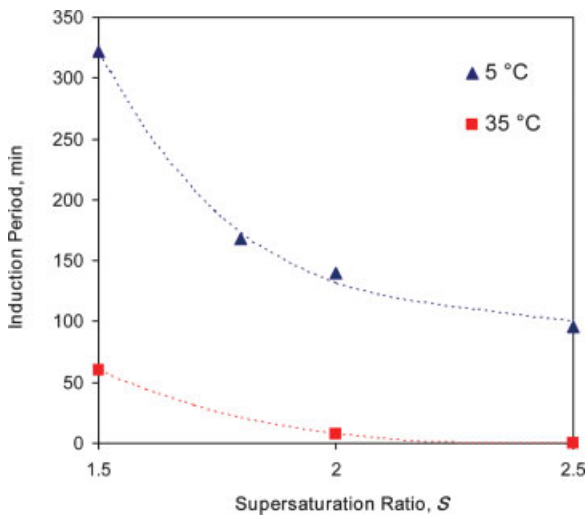

Figure 6. Effect of supersaturation ratio and temperature on induction period.

[Color figure can be viewed in the online issue, which is available at www.interscience.wiley.com.]

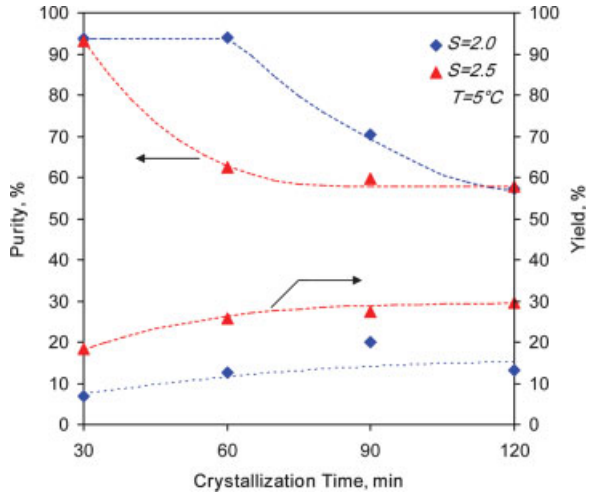

Figure 7. Dependency of product purity and yield on crystallization time for a supersaturated solution of double saturation composition.

[Color figure can be viewed in the online issue, which is available at www.interscience.wiley.com.]

time counting was started when the solutions reached the desired temperature. In a typical experiment, 0.1 g of seeds was used in a solution of volume 100 mL. Solid extraction was performed at different times: 30, 60, 90, and 120 min and the solids were separated from the liquid for purity and yield measurements. The composition of the extracted solids was determined by chiral HPLC. The column was Regis (R,R)-Whelk-O1 and the mobile phase was 2% IPA and 0.2% acetic acid in hexane. The flow rate was 1.5 mL/min. The effect of nonstoichiometric use of resolving agent on resolution was studied using three resolving agent to racemate molar ratios: R values of 1, 0.8, and 0.6.

Influence of Temperature and Supersaturation Ratio on Induction Period. Dependencies of induction period on supersaturation ratio at 5 and 35°C are shown in Figure 6. It can be seen that temperature has a profound influence on induction period. At 35°C, the induction period was exceedingly short for $S > 2$. At $S = 2.5$, the solution readily turned milky before reaching the designated temperature and the induction period was recorded as 0 min. The induction period increased to 7.8 min at $S = 2$ and further to 60 min at $S = 1.5$.

Comparatively, the induction period was much longer under the same supersaturation ratio at 5°C. The induction period was 96 min at $S = 2.5$. It increased gradually to 140 and 168 min at S values of 2 and 1.8, respectively. At $S = 1.5$, it reached 322 min.

These results suggest that seeding should be conducted at a low temperature. The induction period is much longer so that more time is allowed for seeds of NMDG-(S)-IBU to grow. Solutions of S at values of 2 and 2.5 were selected to conduct seeding crystallization.

Seeding in Supersaturated Solution of Double Saturation Composition. Dependencies of purity and yield on crystallization time are shown in Figure 7. Purity is defined as the molar ratio of (S)-IBU to the sum of (R)-IBU and (S)-IBU as observed in the chiral HPLC chromatographs. The yield is defined by the following equation:

$$\text{Yield} = \frac{\text{Amount of solids recovered} \times \text{Purity} - \text{Amount of seeds}}{\text{Amount of NMDG-(S)-IBU present in the supersaturated solution}} \quad (10)$$

The purity of the solid product in a solution of $S = 2.5$ decreased from 94% at 30 min to 62% at 60 min. The solid reached the double saturation composition, 58% at around 90 min. For a solution of $S = 2$, the purity remained at 94% until 60 min. It decreased to 70.4% at 90 min before reaching the double saturation composition at 120 min. It should be noted that NMDG-(R)-IBU precipitation occurred within the measured induction period.

As expected, crystals grew faster in a solution with a higher supersaturation ratio. For a solution of $S = 2.5$, about 18.4% of NMDG-(S)-IBU was recovered at 30 min. The solids were of high purity at 94%. Roughly 30% of NMDG-(S)-IBU was recovered at 120 min but the solids were of poor quality at 58% purity. For a solution of $S = 2$, about 12% of NMDG-(S)-IBU was recovered in highly pure solid form at 94% at 60 min.

The influences of nonstoichiometric use of resolving agent on solid purity and yield are shown in Figure 8. All the solutions were of $S = 2.5$. Very similar patterns can be observed for the three different resolving agent to racemate ratios. However, 100% pure NMDG-(S)-IBU crystals were successfully obtained in a solution of $R = 0.8$ and 0.6 at 30 min; the highest yield of pure product was 22.57% for $R = 0.6$ at 30 min.

Seeding in Supersaturated Solution with Equimolar Composition. It was found that crystal growth was very slow for this composition so that solutions with higher supersaturation ratio (S values of 3 and 4) were used. Dependencies of solid purity and yield on crystallization time are shown in Figure 9. Pure NMDG-(S)-IBU (100%) was recovered at all the crystal-

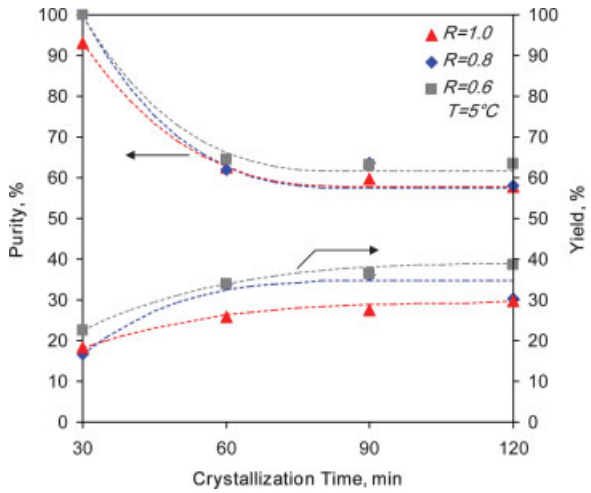

Figure 8. Effect of nonstoichiometric use of resolving agent on product purity and yield for a supersaturated solution of double saturation composition.

[Color figure can be viewed in the online issue, which is available at www.interscience.wiley.com.]

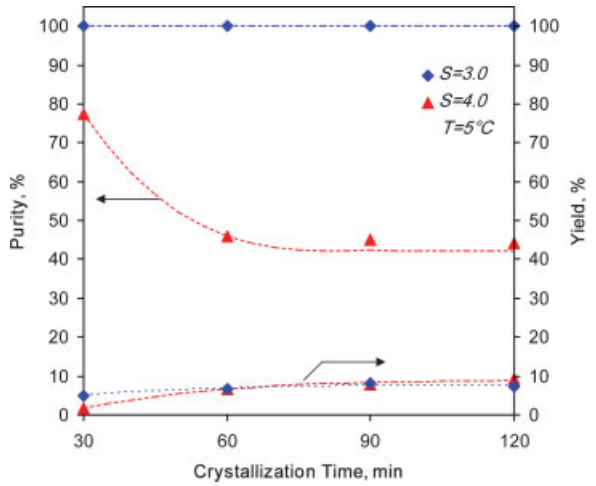

Figure 9. Dependency of product purity and yield on crystallization time for a supersaturated solution with equimolar composition of NMDG-(S)-IBU and NMDG-(R)-IBU.

[Color figure can be viewed in the online issue, which is available at www.interscience.wiley.com.]

lization time studied in the solution of $S = 3$. Solids of only 78% purity were recovered in a solution of $S = 4$ at 30 min and the purity decreased rapidly at longer crystallization times: 46, 45, and 44% at 60, 90, and 120 min, respectively.

The crystals grew slower in solutions of equimolar composition. For solution of $S = 3$, 5% yield of NMDG-(S)-IBU was obtained at 30 min and it increased slightly to 7.4% at 120 min. For a solution of $S = 4$, the yield was roughly 1.7% at 30 min and 9.2% at 120 min.

The influences of nonstoichiometric use of resolving agent on solid purity and yield are shown in Figure 10. All the solutions were of $S = 4$. It can be seen that very similar trends were observed for the three different ratios of resolving agent to racemate. Both product purity and product yield were quite insensitive to the change in the amount of resolving agent used.

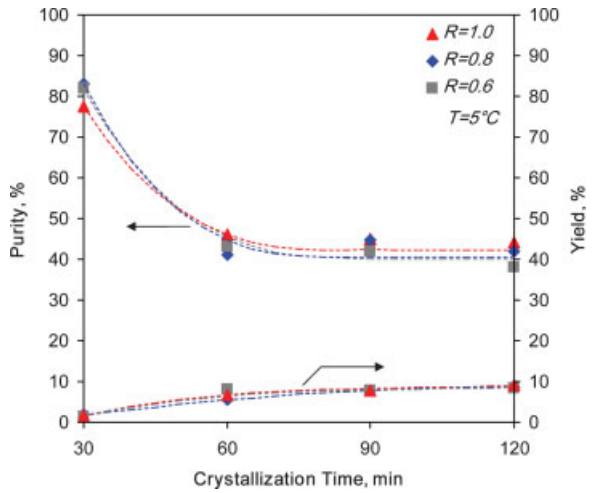

Figure 10. Effect of nonstoichiometric use of resolving agent on product purity and yield for a supersaturated solution with equimolar composition of NMDG-(S)-IBU and NMDG-(R)-IBU.

[Color figure can be viewed in the online issue, which is available at www.interscience.wiley.com.]

Process Synthesis

The SLE and seeding crystallization data are used to synthesize equilibrium-based and seeding-based DSCP. From the Jänecke diagram (Figure 4), a shift in the double saturation composition as Y varies is observed. This shift can be used to design an equilibrium based crystallization process to recover pure NMDG-(S)-IBU.

Figure 11a shows a process flow sheet of a crystallization process to recover pure NMDG-(S)-IBU under equilibrium conditions. The composition change of the process streams is represented on the Jänecke diagram in Figure 11b. Racemic ibuprofen enters the process as the feed (F). It is mixed with the recycled racemic ibuprofen (stream 16) from the racemization unit (R5), solvent (S), and resolving agent NMDG in a reactor (R1) where diastereomeric salts are formed. The solution of diastereomeric salts (stream 2) is mixed with the recycle stream (stream 10) from crystallizer 2 (C2) to become process stream 3. As indicated in Figure 11b, stream 3 is within the saturation compartment of NMDG-(R)-IBU;

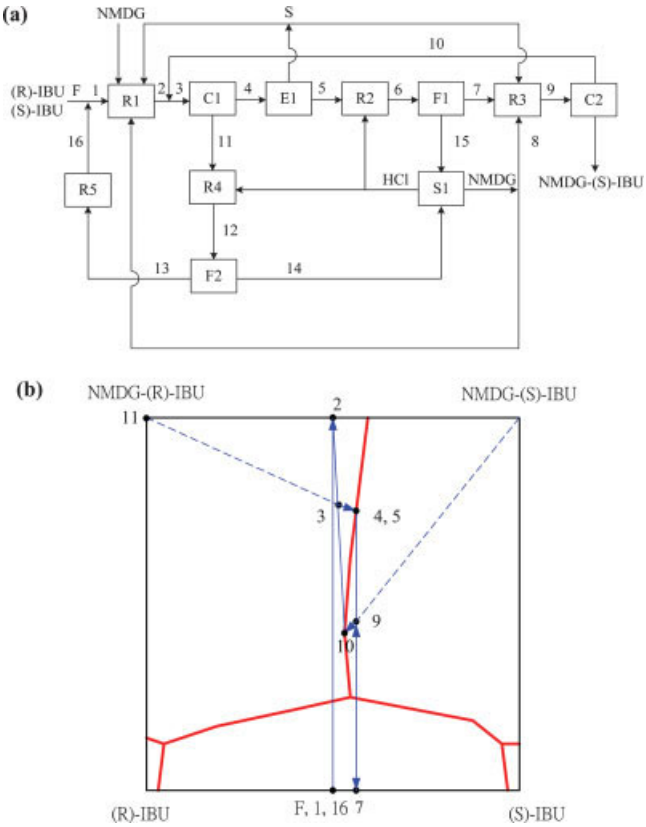

Figure 11. Equilibrium-based crystallization process to recover pure NMDG-(S)-IBU.

(a) Process flow sheet; (b) process paths on the phase diagram. [Color figure can be viewed in the online issue, which is available at www.interscience.wiley.com.]

pure NMDG-(R)-IBU is recovered in the first crystallizer (C1). The crystallization is stopped when the composition of the mother liquor (stream 4) nearly reaches the double saturation curve. The solid and the mother liquor are separated by filtration at the end of crystallization.

In Figure 11b, it can be seen that the amount of resolving agent in the solution has to be decreased in the process stream to pass from the saturation compartment of NMDG-(R)-IBU to that of NMDG-(S)-IBU. This can be accomplished as follows. First, solvent (95 vol % of acetone) is completely evaporated from stream 4 in an evaporator (E1) and the remaining diastereomeric salts (stream 5) react with HCl in a reactor (R2) to liberate ibuprofen in the following reactions:

$$\text{NMDG-(S)-IBU} + \text{HCl} \leftrightarrow \text{NMDGH}^+\text{Cl}^- + \text{(S)-IBU} \quad (11)$$

$$\text{NMDG-(R)-IBU} + \text{HCl} \leftrightarrow \text{NMDGH}^+\text{Cl}^- + \text{(R)-IBU} \quad (12)$$

Our data indicate that the solubility of ibuprofen in water is very low[17]—it will precipitate spontaneously from the solution while $\text{NMDGH}^+\text{Cl}^-$, which is highly soluble in water, remains in solution. Thus, the reactor effluent can be easily separated by filtration into solid ibuprofen (stream 7) and an aqueous solution of $\text{NMDGH}^+\text{Cl}^-$ (stream 15), neglecting the amount of ibuprofen dissolved in water. To recover NMDG from the highly soluble salt, ion exchange resin (S1) can be used.[20] The liberated ibuprofen (stream 7) reacts with some of the recycled NMDG (stream 8) in the presence of solvent (95 vol % of acetone) to form diastereomeric salt solution (stream 9) in reactor R3. Stream 9 is within the saturation compartment of NMDG-(S)-IBU, so that NMDG-(S)-IBU can be recovered in the second crystallizer (C2). The solids and the mother liquor are separated by filtration at the end of crystallization. The solids, NMDG-(S)-IBU, will be subjected to downstream processing to liberate (S)-IBU and the mother liquor (stream 10) is recycled back to C1. The product yield in C2 is about 7.3% based on the lever rule.

For improved process economics, racemization of the NMDG-(R)-IBU in stream 11 is needed. It is known that heating solid (R)-IBU at high temperature under inert environment leads to its racemization.[6] Liberation of (R)-IBU from NMDG-(R)-IBU can be achieved by treating NMDG-(R)-IBU (stream 10) with HCl in R4. As discussed above, the solubility of (R)-IBU is much lower than that of $\text{NMDGH}^+\text{Cl}^-$. The reaction effluent is separated in a filter (F2) and (R)-IBU (stream 12) is fed into the racemization unit (R5), whereas the mother liquor is directed to the ion exchange resin (S1) to recover the NMDG. For simplicity, the amount of ibuprofen present in the aqueous solution of $\text{NMDGH}^+\text{Cl}^-$ (stream 14) is neglected.

By studying the Jänecke diagram, it can be observed that it is not necessary to liberate all the diastereomeric salts in stream 4 to pass from the saturation compartment of NMDG-(R)-IBU to that of NMDG-(S)-IBU. An alternative process is given in Figure 12 based on this observation. Instead, stream 4 is first split into two portions. One portion (stream 16) is fed into R2 to liberate ibuprofen as before. This is represented as movement from point 16 to point 7 as shown in Figure 12b. After liberation, stream 7 is combined with the other portion of the original stream (stream 17) to become

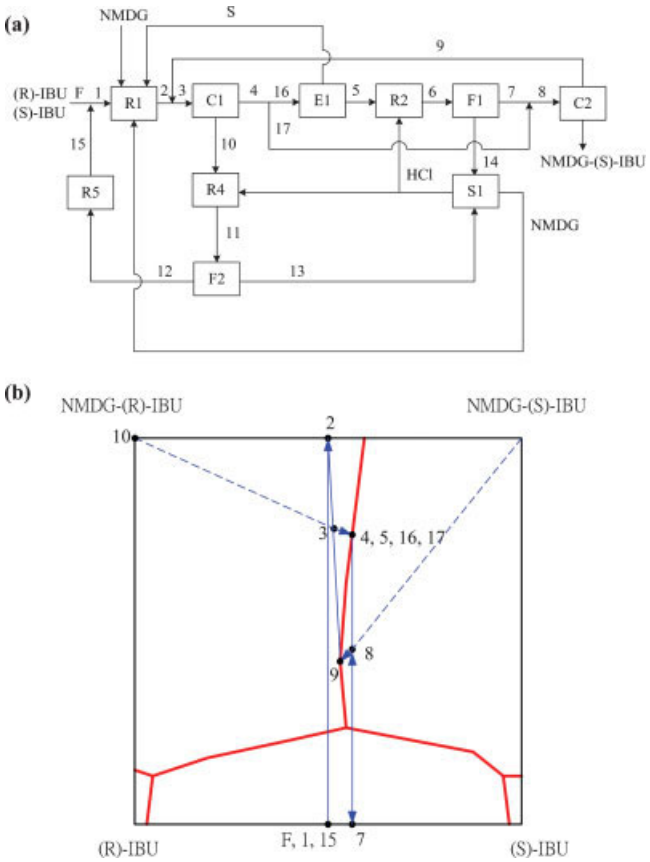

Figure 12. Alternative process.

(a) Process flow sheet; (b) process paths on the phase diagram. [Color figure can be viewed in the online issue, which is available at www.interscience.wiley.com.]

process stream 8. After that, pure NMDG-(S)-IBU can be recovered as before.

In a comparison of the two processes, one observes two advantages of splitting process stream 4. First, we can eliminate one reactor (R3) in the process that is used for reacting the liberated ibuprofen with resolving agent and solvent to form the diastereomeric salts solution again. Second, we can decrease the material loading in R2, F1, and S1, which in turn lead to lower capital and operating costs.

NMDG-(S)-IBU can also be recovered by seeding. The process flow sheet (along with the process paths represented on a Jänecke projection) is shown in Figure 13. Racemic ibuprofen (stream F) mixes with the recycled ibuprofen from the racemization unit (R5) and enters R1 as stream 1. It reacts with NMDG to form diastereomeric salts in the presence of solvent (S). The solution of diastereomeric salts (stream 2) is mixed with the recycle stream (stream 10) from crystallizer 2 (C2) to become process stream 3. As in the equilibrium-based process, NMDG-(R)-IBU is crystallized out from C1 under equilibrium condition and the crystallization is stopped when the mother liquor is about to reach the double saturation composition (stream 4).

The results from the seeding experiments indicate that it is desirable to carry out seeding at the double saturation composition with $R = 0.6$ (Figure 8). To fix the R value of stream 4, the amount of NMDG fed into R1 has to be adjusted. It is

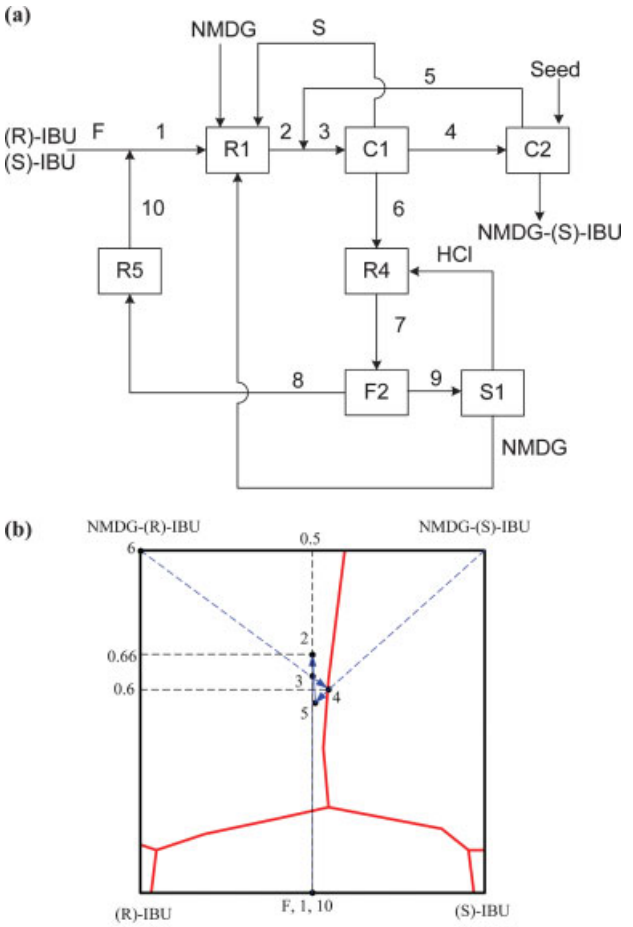

Figure 13. Kinetic-based crystallization process.

(a) Process flow sheet; (b) process paths on the phase diagram. [Color figure can be viewed in the online issue, which is available at www.interscience.wiley.com.]

also related to the yield in C1 and C2 and the composition of the mother liquor in streams 4 and 5. Material balance shows that the amount of NMDG fed into R1 should be 0.66 mole per mole of ibuprofen ($R = 0.66$) as shown in Figure 13b. When crystallization is stopped at the double saturation composition (stream 4), R is exactly equal to 0.6.

In the second crystallizer (C2), the solution is subcooled to 5°C and a small amount of NMDG-(S)-IBU crystals is introduced to the crystallizer for seeding. Based on the bench seeding data, crystallization should be allowed to proceed for 30 min, after which the solids and mother liquor have to be separated. About 22.57% of pure NMDG-(S)-IBU can be recovered.

Alternatively, the process can be simplified by preparing a supersaturated solution of equimolar of NMDG-(R)-IBU and NMDG-(S)-IBU. The alternative process is shown in Figure 14a. Racemic ibuprofen (stream F) mixes with the recycled ibuprofen from the racemization unit (R3) and enters R1 as stream 1. It reacts with NMDG to form diastereomeric salts solution (stream 2) in the presence of solvent (S). By subcooling the solution to 5°C at C1, stream 2 is within the double saturation compartment as shown in Figure 14b. Then seeds of NMDG-(S)-IBU are introduced into the crystallizer (C1) to recover pure NMDG-(S)-IBU as before. Only one crystallizer (C1) is required. However, from the seeding results (Figure 9), considerably lower yield of NMDG-(S)-IBU at C1 is expected.

Conclusions

An integrative approach combining bench-scale experiments, modeling, and conceptual design is proposed for synthesizing diastereomeric salt crystallization processes. This procedure—which includes solvent screening, determination of solid–liquid equilibrium behavior, crystallization by seeding, and process synthesis—is expected to help shorten time for process development. To be concrete, a specific system—the resolution of ibuprofen using NMDG as resolving agent—has been studied in some detail, although both the procedure and the companion experimental techniques are generic in nature.

The solid–liquid equilibrium phase diagram plays a key role in this approach. By identifying the size and location of each crystallization compartment, it is possible for the engineer to conceptualize a process to recover the desired enantiomer. The entire process including formation of the diastereomeric salts, separation of these salts by crystallization, racemization, and recovery of the enantiomer can be visualized in

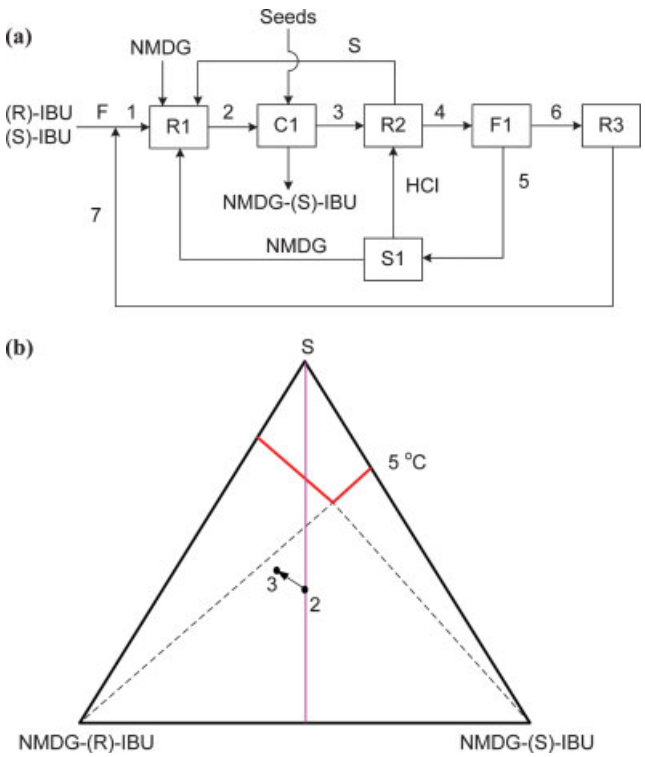

Figure 14. A kinetic-based crystallization process with resolution conducted at equimolar composition.

(a) Process flow sheet; (b) process paths on the phase diagram. [Color figure can be viewed in the online issue, which is available at www.interscience.wiley.com.]

the form of process paths on the phase diagram. In addition to equilibrium-based crystallization, the extent of crystallization under kinetically controlled conditions can be similarly represented. The difference is that the process path of the former is limited by the crystallization boundaries, whereas that of the latter is governed by crystallization kinetics. Also, thermodynamically controlled crystallization is usually more reliable, whereas kinetically controlled crystallization may offer separation that cannot be achieved otherwise.

The solid–liquid equilibrium data can be measured using the isothermal method. By determining the solubility of the various salts and enantiomers at different points of the composition space, an isobaric–isothermal phase diagram is constructed. Crystallization by seeding is quantified by yield and purity as a function of supersaturation ratio, crystallization temperature, and time for crystallization. Note that the starting point of a kinetically controlled process path is determined by the composition of the feed to the crystallizer, whereas its end point is determined by the purity and yield of the crystal product. Thus, this experimental approach avoids the complications of measuring crystallization nucleation and growth kinetics.

This study is limited to a preliminary conceptual design. To verify its feasibility, it is necessary to study such investigative areas as racemization kinetics, solvent and resolving agent recovery, crystal filtration, and washing.[21,22] Efforts in these directions are under way.

Notation

c = solute concentration, g/mL
c* = saturation concentration, g/mL
R = molar ratio of resolving agent to the racemate
S = supersaturation ratio
X = anionic coordinate
Y = cationic coordinate

Literature Cited

1. Rouhi AM. Chiral business. *Chem Eng News*. 2003;81:45–55.
2. Bhushan R, Martens J. Resolution of enantiomers of ibuprofen by liquid chromatography: A review. *Biomed Chromatogr*. 1998;12: 309–316.
3. Collins AN, Sheldrake GN, Crosby J, eds. *Chirality in Industry II: Developments in the Manufacture and Applications of Optically Active Compounds*. West Sussex, UK: John Wiley & Sons; 1992.
4. Tung HH, Waterson S, Reynolds SD. *Formation and Resolution of Ibuprofen Lysinate*. U.S. Patent Number 4 994 604; 1991.
5. Tung HH, Waterson S, Reynolds SD, Paul E. Resolution of ibuprofen via stereospecific crystallization. *AIChE Symp Ser*. 1991; No. 284.
6. Bhattacharya A. Temperature selective diastereo-recognition (TSD): Enantiomeric ibuprofen via environmentally benign selective crystallization. *Org Process Res Dev*. 2003;7:717–722.
7. Schlomer G, Lodewijk E, Withers G. *Resolution of Ibuprofen*. U.S. Patent Number 5 621 140; 1994.
8. Nohira H. *Optical Resolution of (±)-2-(4-Isobutylphenyl)-Propionic Acid*. U.S. Patent Number 5 321 154; 1994.
9. Kozma D, ed. *CRC Handbook of Optical Resolutions via Diastereomeric Salt Formation*. Boca Raton, FL: CRC Press; 2001.
10. Schroer JW, Wibowo C, Ng KM. Synthesis of chiral crystallization processes. *AIChE J*. 2001;47:369–388.
11. Wilen SH, Collet A, Jacques J. Strategies in optical resolutions. *Tetrahedron*. 1977;33:2725–2736.
12. Jacques J, Collet A, Wilen SH. *Enantiomer, Racemates, and Resolutions*. New York: Wiley; 1981.
13. Wibowo C, Ng KM. Unified approach for synthesizing crystallization-based separation processes. *AIChE J*. 2000;46:1400–1421.
14. Samant KD, Ng KM. Representation of high-dimensional solid–liquid phase diagrams of ionic systems. *AIChE J*. 2001;47:861–879.
15. Fuyuhiro A, Yamanari K, Shimura Y. Solubility isotherms of reciprocal salt-pairs of optically active cobalt (III) complexes. *Bull Chem Soc Jpn*. 1979;52:90.
16. Kowk KS, Chan HC, Chan CK, Ng KM. Experimental determination of solid–liquid equilibrium phase diagrams for crystallization-based process synthesis. *Ind Eng Chem Res*. 2005;44:3788–3798.
17. Lam WH. *Chiral Resolution by Diastereomeric Salt Crystallization*. MPhil Thesis. Hong Kong University of Science and Technology; 2005.
18. Lancia A, Musmarra D, Prisciandaro M. Measuring induction period for calcium sulfate dihydrate precipitation. *AIChE J*. 1999;45:390–397.
19. Mullin JW. *Crystallization*. 4th Edition. Oxford, UK: Butterworth-Heinemann; 2001.
20. Nieuwenhuijzen J. *Resolutions with Families of Resolving Agents: Principles and Practices*. PhD Thesis. Groningen, The Netherlands: University of Groningen; 2002.
21. Chang WC, Ng KM. Synthesis of the processing system around a crystallizer. *AIChE J*. 1998;44:2240–2251.
22. Wibowo C, Chang WC, Ng KM. Design of integrated crystallization systems. *AIChE J*. 2001;47:2574–2492.

Manuscript received May 7, 2006, and revision received Nov 11, 2006.